

See discussions, stats, and author profiles for this publication at: <https://www.researchgate.net/publication/263959142>

Structure-Directing Effect of Organic Cations in the Assembly of Anionic In(III)/Diazinedicarboxylate Architectures

ARTICLE in CRYSTAL GROWTH & DESIGN · FEBRUARY 2012

Impact Factor: 4.89 · DOI: 10.1021/cg201572y

CITATIONS

18

READS

17

6 AUTHORS, INCLUDING:



Javier Cepeda

Universidad del País Vasco / Euskal Herriko U...

33 PUBLICATIONS 280 CITATIONS

[SEE PROFILE](#)



Garikoitz Beobide

Universidad del País Vasco / Euskal Herriko U...

54 PUBLICATIONS 715 CITATIONS

[SEE PROFILE](#)



Oscar Castillo

Universidad del País Vasco / Euskal Herriko U...

133 PUBLICATIONS 1,972 CITATIONS

[SEE PROFILE](#)



Pascual Roman

Universidad del País Vasco / Euskal Herriko U...

192 PUBLICATIONS 3,063 CITATIONS

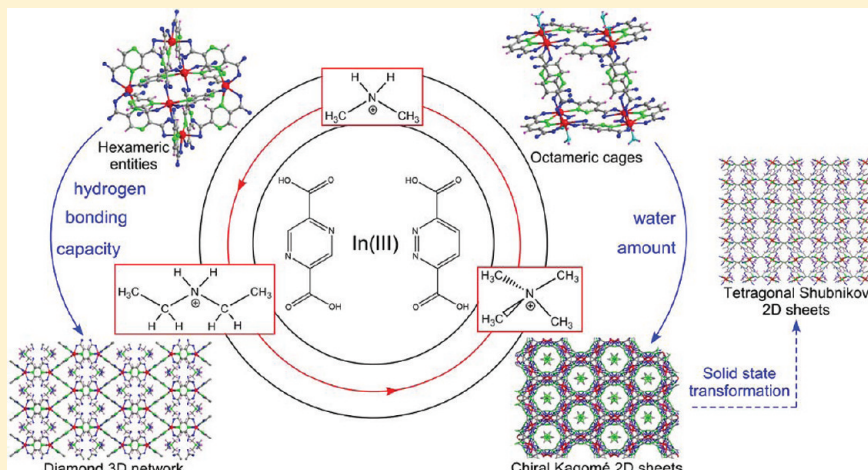
[SEE PROFILE](#)

Structure-Directing Effect of Organic Cations in the Assembly of Anionic In(III)/Diazinedicarboxylate Architectures

Javier Cepeda, Garikoitz Beobide,* Oscar Castillo,* Antonio Luque, Sonia Pérez-Yáñez, and Pascual Román

Departamento de Química Inorgánica, Facultad de Ciencia y Tecnología, Universidad del País Vasco (UPV/EHU), Apartado 644, E-48080 Bilbao, Spain

Supporting Information



ABSTRACT: We report herein the synthesis and physicochemical characterization of seven new indium-pyrazine-2,5-dicarboxylato (pzdc) and pyridazine-3,6-dicarboxylato (pddc) compounds: $(\text{dma})_6[\text{In}_6(\mu\text{-pzdc})_{12}] \cdot x\text{H}_2\text{O}$ (**1**), $(\text{dea})_6[\text{In}_6(\mu\text{-pzdc})_{12}] \cdot x\text{H}_2\text{O}$ (**2**), $\{\text{(tma)}[\text{In}(\mu\text{-pzdc})_2]\cdot 2\text{H}_2\text{O}\}_n$ (**3**), $\{\text{(dea)}[\text{In}(\mu\text{-pzdc})_2]\cdot 2\text{H}_2\text{O}\}_n$ (**4**), $\{\text{(dma)}[\text{In}(\mu\text{-pddc})_2]\cdot x\text{H}_2\text{O}\}_n$ (**5**), $\{\text{(dma)}[\text{In}(\mu\text{-pddc})_2]\}_n$ (**6**), and $(\text{dma})_4[\text{In}_8(\mu\text{-pddc})_{12}(\text{H}_2\text{O})_8(\text{OH})_4] \cdot x\text{H}_2\text{O}$ (**7**) (where dma = dimethylammonium, dea = diethylammonium, tma = tetramethylammonium). Two types of $\text{In}(\text{III})/\text{pzdc}$ structures have been obtained. The first one (**1** and **2**) is comprised of discrete hexanuclear anionic assemblies held together by hydrogen bonding interactions through the organic cations generated by the thermal hydrolysis of the amide solvents. The second one (**3** and **4**) consists of an anionic three-dimensional (3D) framework with channels that are occupied by the counterions and solvent molecules. The first type of structure seems to be the kinetically preferred one since it is obtained when using relatively soft solvothermal conditions (120 °C) and counterions that are able to establish relatively strong hydrogen bonding interactions. The 3D frameworks crystallize when the organic counterion is unable to establish hydrogen bonding interactions or when employing a higher temperature (150 °C). The metal-organic assemblies obtained in the $\text{In}(\text{III})/\text{pddc}$ system range from two-dimensional (2D) sheets (**5** and **6**) to discrete octameric entities (**7**) depending on the amount of water in the reaction mixture. It is worth noting that the open lamellar crystal structure of compound **5** undergoes a solid state transformation accompanied by the release of water molecules, rendering the solvent free 2D architecture of **6** that exhibits a different connectivity. Surprisingly, a prolonged exposure of **6** to a water saturated atmosphere does not revert to **5** but promotes a partial and reversible transformation to give a new unidentified $\text{In}-\text{pddc}$ compound.

INTRODUCTION

In metal-ligand directed assembly, the molecular building block approach has been adopted for the synthesis of functional metal-organic assemblies (MOAs) which range from discrete metal-organic polyhedra (MOPs) to three-dimensional (3D) frameworks (MOFs).¹ Until now, most contributions have focused primarily on the use of nodes such as isolated transition-metal centers² or clusters.^{3,4} We have selected the $\text{In}(\text{III})$ metal center owing to its variable coordination

geometry and also because MOAs from p-block metals are rare. For example, it can form a four-connected $\{\text{In}(\text{O}_2\text{CR})_4\}$ group, which is an appealing tetrahedral node for targeting zeolite-type MOFs and MOPs.⁵ Moreover, some of these compounds based on indium and polycarboxylic aromatic

Received: November 28, 2011

Revised: January 24, 2012

Published: January 27, 2012



ligands present interesting features such as luminescence, permanent porosity, and catalysis.^{5d,6} To date much of the work with In(III) systems has been focused mainly on aromatic carboxylic ligands and little attention has been paid to nitrogen-donor multicarboxylate ligands.^{7,8} One of our research lines is devoted to the study of diazines functionalized with carboxylate groups, because the coordination to a metal center is ensured by the formation of a five-member chelate ring involving the imine nitrogen atom and the adjacent carboxylic oxygen atom.^{5d,9} Therefore, we have chosen pyrazine-2,5-dicarboxylate and pyridazine-3,6-dicarboxylate acids as linkers to build In(III) MOAs and to explore the opportunities given by the different angular dispositions of the two chelating sides of the dicarboxylic diazines.

We have performed a study of the preferred coordination geometries and coordination modes registered in the CSD database¹⁰ in order to clarify the coordination characteristics of the indium(III)/ α -carboxylic azine systems (Figure 1). In spite

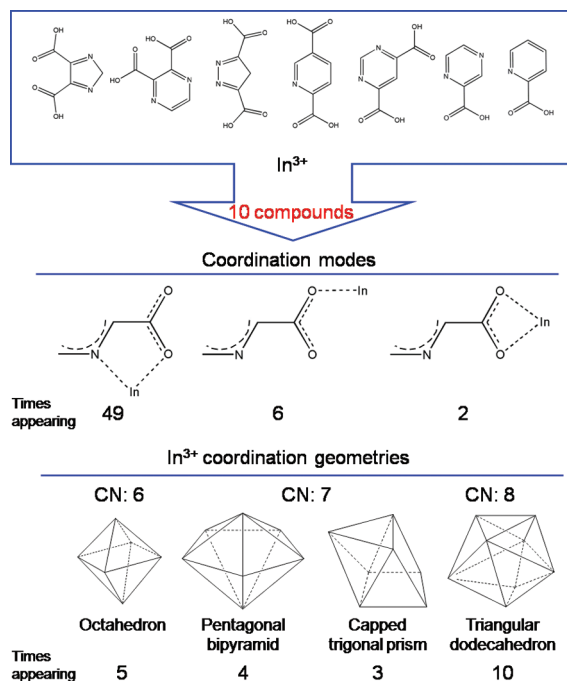


Figure 1. Coordination modes and geometries in indium(III) and α -carboxylic azine/diazine systems.

of the small number of examples, the chelating coordination mode involving the imine nitrogen atom and the adjacent carboxylate oxygen atom seems to be the preferred one, so that the most probable coordination modes for the diazinedicarboxylate ligands would be those involving this chelating ring (Figure 2). However, other structural and geometric features such as the relative disposition of the metal centers and/or the presence of the additional ligands can alter the predicted preferred order of the bridging modes. In the present paper, we report seven indium/diazinedicarboxylate compounds that present MOAs ranging from discrete clusters to extended 3D frameworks and all of them exhibit bridging ligands with at least one chelating pentagonal ring (A, B, and C modes), except one of the diazine bridging ligands of compound 7 which is coordinated in bis-monodentate mode (D).

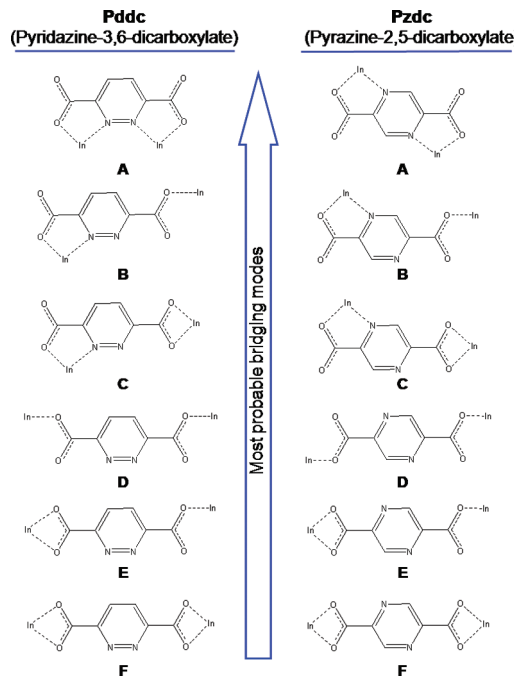


Figure 2. Probable coordination modes of the employed ligands.

EXPERIMENTAL SECTION

Syntheses. All the chemicals were reagent grade and were used as commercially obtained. The starting material pyridazine-3,6-dicarboxylic acid (H_2pddc) was prepared following the previously reported procedure.¹¹ Data concerning to the elemental analyses and infrared spectra are given in the Supporting Information.

$\{(dma)_6In_6(\mu-pzdc)_{12}\} \cdot xH_2O$ (**1**) and $\{(dea)_6In_6(\mu-pzdc)_{12}\} \cdot xH_2O$ (**2**). A total of 0.0225 g of indium nitrate (0.075 mmol) and 0.0306 g of pyrazine-2,5-dicarboxylic acid (0.150 mmol) were dissolved in 25 mL of a dimethylformamide (DMF)/methanol mixture (1:1) for **1** and 25 mL of diethylformamide (DEF) for **2**. Colorless single-crystals were obtained by placing the resulting solutions on a 45 mL Teflon-lined stainless steel autoclave under autogenous pressure at 120 °C during 3 days and then slowly cooling down to room temperature (2 °C/h). The compounds decomposed upon removal from the mother liquid to yield an amorphous phase.

$\{(tma)_6In(\mu-pzdc)_2\} \cdot 2H_2O$ (**3**). Single crystals of **3** were obtained following the same procedure of **1**, but adding also 0.075 mmol of tetramethylammonium bromide (0.0117 g) to the DMF/MeOH mixture. High-purity polycrystalline samples of **3** can be generated by adding the reactants directly in stoichiometric quantities and letting the resulting solution to stir during 3 h at 80 °C.

$\{(dea)_6In(\mu-pzdc)_2\} \cdot 2H_2O$ (**4**). Crystals of **4** were obtained following the same procedure of **2**, but setting the solvothermal temperature at 150 °C.

$\{(dma)_6In(\mu-pddc)_2\} \cdot xH_2O$ (**5**). A total of 0.0225 g of indium nitrate (0.075 mmol) dissolved in 3 mL of DMF were added dropwise to 15 mL of a DMF solution containing 0.0276 g of pyridazine-3,6-dicarboxylic acid (0.150 mmol) and then the resulting mixture was left at room temperature. Well-formed trigonal antiprism shaped crystals of **5** appeared after one week.

$\{(dma)_6In(\mu-pddc)_2\}_n$ (**6**). The addition of 8.2 μ L of aniline (0.150 mmol) to the solution of **5** led to the formation of single crystals of **6** after keeping the solution at room temperature for 2 months. High purity polycrystalline samples of **6** can also be easily obtained from compound **5** due to its spontaneous solid state transformation after their removal from the mother liquid. The exposure of compound **6** to a water saturated atmosphere during a week led to a partial and reversible transformation to a new unidentified compound that presents a different X-ray powder diffraction pattern.

$(dma)_4[In_8(\mu-pzdc)_{12}(H_2O)_8(OH)_4] \cdot xH_2O$ (**7**). A procedure similar to that described for the synthesis of compound **5** but in a water/DMF (3:1) mixture led to the growth of well-shaped crystals of **7** after five days. Compound **7** suffers a slow loss of crystallinity upon removal from the mother liquid.

Physical Measurements. Elemental analyses (C, H, N) were performed on an Euro EA Elemental Analyzer, whereas the metal content was determined by an inductively coupled plasma atomic emission spectrometer (ICP-AES) from Horiba Yobin Yvon Activa. The IR spectra (KBr pellets) were recorded on a FTIR 8400S Shimadzu spectrometer in the 4000–400 cm⁻¹ spectral region. Thermal analyses (TG/DTA) were performed on a TA Instruments SDT 2960 thermal analyzer in a synthetic air atmosphere (79% N₂/21% O₂) with a heating rate of 5 °C·min⁻¹.

X-ray Diffraction Data Collection and Structure Determination. The single crystal X-ray diffraction data collections were done at 293(2) K for **1** and at 100(2) K for compounds **2–6** on Oxford Diffraction Xcalibur (**1**, **3–6**; $\lambda_{Mo-K\alpha} = 0.71073$ Å) and STOE IPDS (**2**; $\lambda_{Mo-K\alpha} = 0.71073$ Å) diffractometers with graphite-monochromated radiation, and at 100(2) K on Agilent Technologies Supernova diffractometer ($\lambda_{Cu-K\alpha} = 1.5418$ Å) for compound **7**. Crystals of compound **1** suffer a fast degradation when removing them from the mother liquid, so prior to data acquisition they had to be mounted in a 0.1 mm diameter Lindemann capillary with the mother liquid. The data reduction was done with the CrysAlisPro and X-RED programs, respectively.¹² All the structures were solved by direct methods using the SIR92 program¹³ and refined by full-matrix least-squares on F² including all reflections (SHELXL97).¹⁴ All calculations were performed using the WINGX crystallographic software package.¹⁵ After completing the initial structure solution, the difference Fourier map for compounds **1**, **2**, **5**, and **7** showed the presence of substantial electron density at the voids of the structures that was impossible to model. Therefore, its contribution was subtracted from the reflection data by the SQUEEZE method¹⁶ as implemented in PLATON.¹⁷ Some of the atoms of the cations in compounds **1**, **2**, **4**, **5**, and **7** are disordered and present a significantly high atomic displacement parameter, so they have been isotropically refined with the inclusion of some additional parameters to fit their distances to the mean values encountered in the CSD database for nondisordered cations. Crystal parameters and details of the final refinements of compounds **1–7** are summarized in Table 1. The X-ray powder diffraction (XRPD) patterns were collected at 25 °C on a Phillips XPERT powder diffractometer with Cu-K α radiation ($\lambda = 1.5418$ Å) over the range 5 < 2θ < 50° (for **5**) and 10 < 2θ < 50° (**6**) with a step size of 0.02° and an acquisition time of 2.5 s per step. Indexation of the diffraction profiles were made by means of the FULLPROF program (pattern-matching analysis)¹⁸ on the basis of the space group and the cell parameters found by single crystal X-ray diffraction. The calculated and observed diffraction patterns are shown in the Supporting Information. Variable-temperature X-ray powder diffraction measurements of compounds **5** and **6** were run under ambient atmosphere with a heating rate of 5 °C·min⁻¹ and measuring a complete diffractogram every 20 °C.

RESULTS AND DISCUSSION

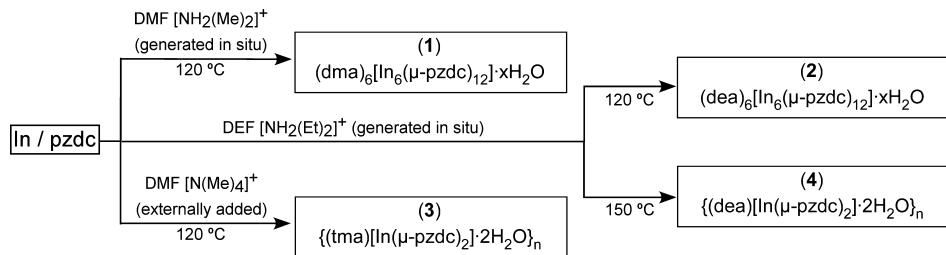
Comments on the In(III) and pzdc/pzdc Systems. Two different types of MOAs have been obtained for the pzdc complexes. The first one (**1** and **2**) is comprised of discrete octahedral anionic assemblies that are held together by hydrogen bonding interactions through organic counterions generated by the thermal hydrolysis of the amide solvent (DMF/DEF). The second one (**3** and **4**) consists of a 3D framework with channels that are occupied by organic cations and solvent molecules. The first type of MOA seems to be the kinetically preferred one as it is obtained when applying relatively soft solvothermal conditions (120 °C) together with counterions such as dimethylammonium and diethylammonium cations that are able to establish relatively strong

Table 1. Crystallographic Data and Structure Refinement Details of Compounds 1–7

	1	2	3	4	5	6	7
empirical formula	$C_{14}H_{12}InN_5O_8 \cdot xH_2O$	$C_{16}H_{16}InN_5O_8 \cdot 2H_2O$	$C_{16}H_{16}InN_5O_8 \cdot 2H_2O$	$C_{16}H_{16}InN_5O_8 \cdot 2H_2O$	$C_{14}H_{12}InN_5O_8 \cdot xH_2O$	$C_{14}H_{12}InN_5O_8$	$C_{10}H_9InN_5O_7 \cdot xH_2O$
formula weight	493.09 ^a	521.15 ^a	557.19	557.19	493.09 ^a	493.09	413.52 ^a
crystal system	trigonal	cubic	tetragonal	monoclinic	trigonal	orthorhombic	orthorhombic
space group	$R\bar{3}$	$P\bar{a}\bar{3}$	$I4_1/a$	$C2/c$	$R\bar{3}c$	$Aba2$	$Pbc\bar{a}$
<i>a</i> (Å)	20.962(3)	31.4338(9)	9.159(3)	10.828(1)	15.380(1)	12.928(2)	21.2339(1)
<i>b</i> (Å)	20.962(3)	31.4338(9)	9.159(3)	17.083(1)	15.380(1)	10.806(2)	28.3875(1)
<i>c</i> (Å)	32.498(5)	31.4338(9)	24.445(14)	11.467(1)	52.911(1)	12.262(3)	28.7497(2)
β (°)				106.84(1)			
<i>V</i> (Å ³)	12367(5)	31059(3)	2050.6(15)	2030.7(2)	10839.0(16)	1713.0(6)	17329.67(16)
<i>Z</i>	18	48	4	4	18	4	32
GOF ^b	0.853	0.900	0.943	1.008	1.114	1.008	1.079
<i>R</i> _{int}	0.0885	0.0896	0.0430	0.0342	0.0215	0.0349	0.0360
final <i>R</i> indices							
$[I > 2\sigma(I)] R_1^c / wR_2^d$	0.0547/0.1194	0.0598/0.1611	0.0313/0.0698	0.0511/0.1239	0.0416/0.1296	0.0306/0.0723	0.0317/0.0873
all data R_1^c / wR_2^d	0.1136/0.1278	0.0802/0.1695	0.0480/0.0728	0.0644/0.1296	0.0496/0.1339	0.0379/0.0739	0.0347/0.0889

^aFormula weights calculated without crystallization water molecules, ^bS = $[\sum w(F_0^2 - F_c^2)^2 / (N_{obs} - N_{param})]^{1/2}$, ^cR₁ = $\sum ||F_0|| - |F_c| / \sum ||F_0||$, ^dwR₂ = $[\sum w(F_0^2 - F_c^2)^2 / \sum wF_0^2]^{1/2}$; $w = 1 / [\sigma^2(F_0^2) + (aP)^2]$ + b where $P = (\max(F_0^2, 0) + 2F_c^2)/3$ with $a = 0.0629$ (**1**), 0.1144 (**2**), 0.0402 (**3**), 0.0793 (**4**), 0.0847 (**5**), 0.0459 (**6**) and 0.0421 (**7**); $b = 29.5052$ (**5**) and 36.9325 (**7**).

Scheme 1. Synthetic Conditions on the In/pzdc System



Scheme 2. Transformations between In/pddc Complexes

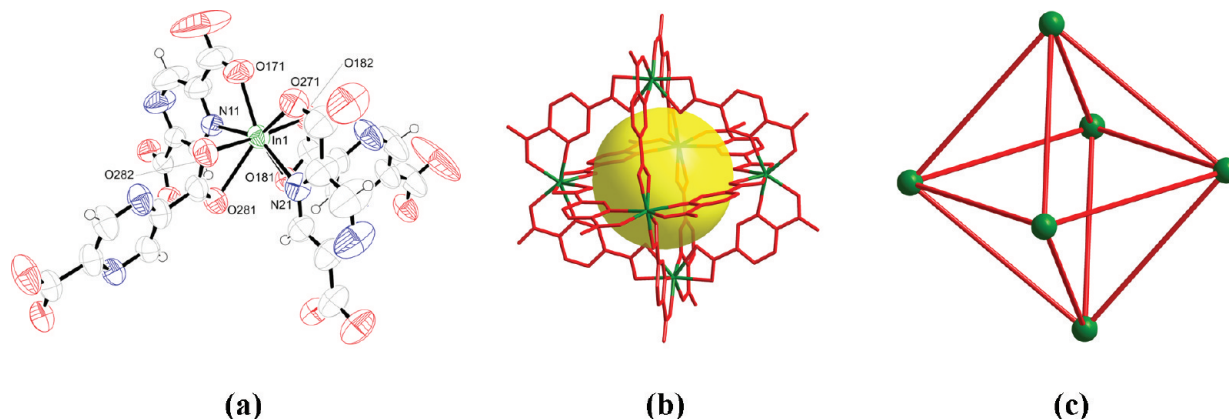
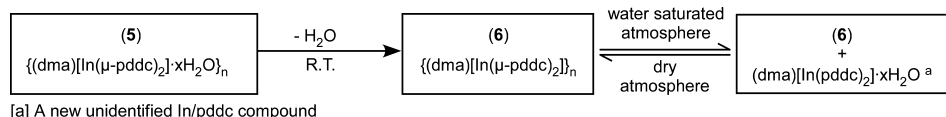


Figure 3. (a) Illustration of the molecular $\text{InN}_2(\text{CO}_2)_4$ building block in compound 1. (b) Void inside the octahedron cage. (c) Schematic representation of the octahedron.

hydrogen bonding interactions that ensure the crystallization of the hexameric discrete assemblies. A 3D framework (4) is obtained using DEF as the solvent and setting the reaction temperature at 150 °C, probably because a partial or total solubilization of the octahedral assemblies takes place allowing the system to evolve toward the thermodynamically preferred product. The stronger hydrogen bonding donor capacity of the dimethylammonium cation (because of the higher N–H bond polarization with respect to the diethylammonium cation) precludes the transition toward the 3D structure in the studied temperature range (≤ 180 °C). Further evidence is derived when using an organic cation unable to establish hydrogen bonding interactions such as tetramethylammonium, whose presence in the reaction media forces the 3D structure (3) to be formed whatever the temperature employed. Scheme 1 shows the synthetic conditions to afford compounds 1–4.

The use of solvothermal conditions in the In(III)/pddc system does not provide any advantage as all reagents remain dissolved when opening the reaction vessel, so that the pddc compounds were synthesized at room temperature. The assemblies present in these compounds range from discrete octameric entities to two-dimensional (2D) sheets depending on the water content in the reaction mixture and on the presence of structure directing agents such as aniline. The use of a 3:1 water/DMF mixture allows the simultaneous occurrence of a significant concentration of dimethylammonium cations and hydroxide anions in the reaction media. The

presence of OH^- anions generates discrete octameric entities with μ -hydroxido bridges and the dimethylammonium cations ensure the stability of the crystal building (7). On the other hand, when using DMF without further purification a lamellar structure is obtained (5), in which crystallization water molecules coming from the solvent impurities or ambient humidity are embedded among the $[\text{In}(\mu\text{-pddc})_2]_n$ sheets. The removal of this latter compound from the mother liquid leads to a spontaneous solid state transformation that provides an anhydrous polycrystalline compound (6). Surprisingly, the addition to the reaction media of an apparently innocent molecule such as aniline seems to seize, by means of hydrogen bonding interactions, the small amount of water impurities. In this way, it provides an easy route that allowed us to get single crystals of 6. Its X-ray characterization shows again a lamellar crystal structure but its connectivity within the sheet is different. This latter compound undergoes a partial and reversible transformation to give a new unidentified compound upon exposure to a water saturated atmosphere. Scheme 2 summarizes the structural transformations between the indium/pddc compounds.

Structural Description of $(\text{dma})_6[\text{In}_6(\mu\text{-pzdc})_{12}] \cdot x\text{H}_2\text{O}$ (1) and $(\text{dea})_6[\text{In}_6(\mu\text{-pzdc})_{12}] \cdot x\text{H}_2\text{O}$ (2). These compounds consist of discrete $[\text{In}_6(\text{pzdc})_{12}]^{6-}$ entities that are linked together by an extensive hydrogen bonding network provided by the organic counterions, which are generated during the thermal hydrolysis of the DMF and DEF solvents, respec-

Table 2. Selected Bond Lengths (\AA) of Compounds 1 and 2^a

Compound 1	Compound 2				
In1–N11	2.375(5)	In1–N11	2.395(5)	In2–N31	2.359(7)
In1–N21	2.403(5)	In1–N21	2.381(5)	In2–N41	2.349(5)
In1–O171	2.202(4)	In1–O171	2.201(5)	In2–O281	2.202(7)
In1–O181a	2.199(4)	In1–O181c	2.248(4)	In2–O282	2.427(5)
In1–O182a	2.481(4)	In1–O182c	2.377(4)	In2–O371	2.194(6)
In1–O271	2.181(4)	In1–O271	2.221(4)	In2–O471	2.198(5)
In1–O281b	2.252(4)	In1–O481d	2.222(4)	In2–O381c	2.203(7)
In1–O282b	2.342(4)	In1–O482d	2.509(4)	In2–O382c	2.541(5)

^aSymmetry codes: (a) $-y + 1, x - y, z$; (b) $y + 1/3, -x + y + 2/3, -z + 2/3$; (c) y, z, x ; (d) z, x, y .

tively.¹⁹ The anionic metal–organic assembly (Figure 3) is composed of six In(III) atoms that occupy the vertexes of an octahedron, whose edges are formed by 12 nonsymmetric bischelating $\mu\text{-pzdc}\cdot\kappa^2N,O:\kappa^2O',O''$ ligands (bridging C mode in Figure 2) with an In…In distance of ca. 8.4 \AA . The In…In angles are almost 60° and 90° like in the ideal octahedron. The cluster possesses an internal cavity with an approximate diameter of 4 \AA which is accessible through eight triangular windows with a diameter of ca. 2 \AA . Selected bond lengths for the coordination polyhedra of 1 and 2 are gathered in Table 2. The indium atom shows a slightly distorted triangular dodecahedron geometry ($S_{DD} = 2.21$ for 1 and $S_{DD} = 2.51$ for 2)²⁰ in which four pzdc ligands are chelating the metal center, two of them through the α -carboxylato imine site and the other ones by means of the carboxylate group.

The crystal packing of these compounds is governed by the hydrogen bonding network established by the organic cations that act as structure directing agents. In compound 1, six dimethylammonium cations are placed near the pzdc edges to interconnect two cluster entities by means of double symmetric O271…H–N32–H…O181 interactions (Figure 4), in such a way that each anionic cluster is surrounded by six others preserving their relative orientation to give a six-connected uninodal net possessing the pcu topology and the (4¹².6³) point symbol. This anion–cation packing presents a high free volume of 45.2% of the total unit cell volume,¹⁷ occupied by crystallization water molecules. The discrete clusters of compound 2 are joined through two crystallographically different diethylammonium cations by means of two hydrogen bonding pathways (O272…H–N63–H…O371/O471 and O171/O172…H–N53–H…N44/O481), forcing the neighboring octahedral anions to change their disposition and allowing each cluster to be surrounded by other 12 ones (Figure 5). This arrangement results in a net with the (3²¹.4³³.5¹²) point symbol, which is a new topology that has been registered as jcr3 in the TTD database.²¹ The supramolecular assembling of the discrete entities leads to a free volume of 32.0% per unit cell which is filled by water molecules. Compounds 1 and 2 exhibit voids with different features. The isolated voids sited inside the hexameric entities are surrounded by an intricate 3D network of interconnected microchannels in 1, whereas the outer solvent accessible space in 2 is segregated in discrete voids that are not connected among them. The supramolecular interactions of compounds 1 and 2 are not strong enough to retain the crystallinity once the single-crystals are removed from the mother liquids, as they render amorphous products.

Structural Descriptions of {(tma)[In(μ -pzdc)]₂}·2H₂O_n (3) and {(dea)[In(μ -pzdc)]₂}·2H₂O_n (4)}. Compounds 3 and 4 show a 3D anionic indium(III)-pzdc framework with embedded crystallization water molecules and organic counterions. The

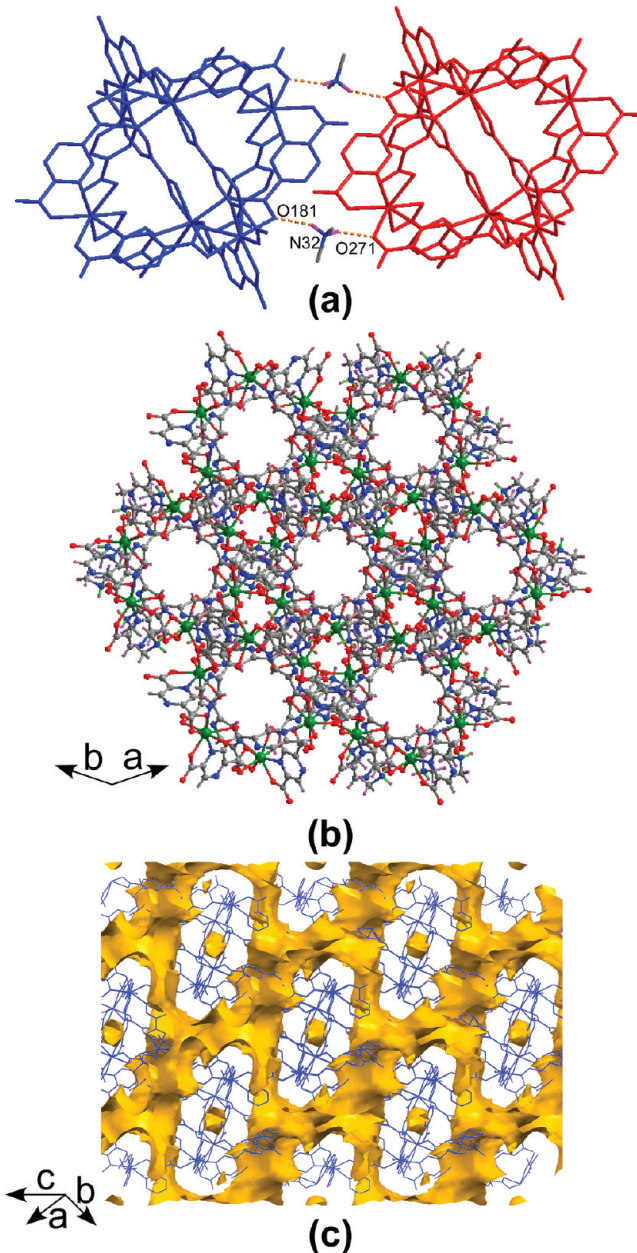


Figure 4. Crystal structure of 1: (a) supramolecular interactions, (b) packing along the c axis, and (c) solvent accessible surface (probe radius = 1.4 \AA , the organic counterions have not been removed).

metal–organic network is formed by pseudotetrahedral $\text{InN}_4(\text{CO}_2)_4$ building units in which the metal center is octacoordinated to the nitrogen atoms and to the carboxylato

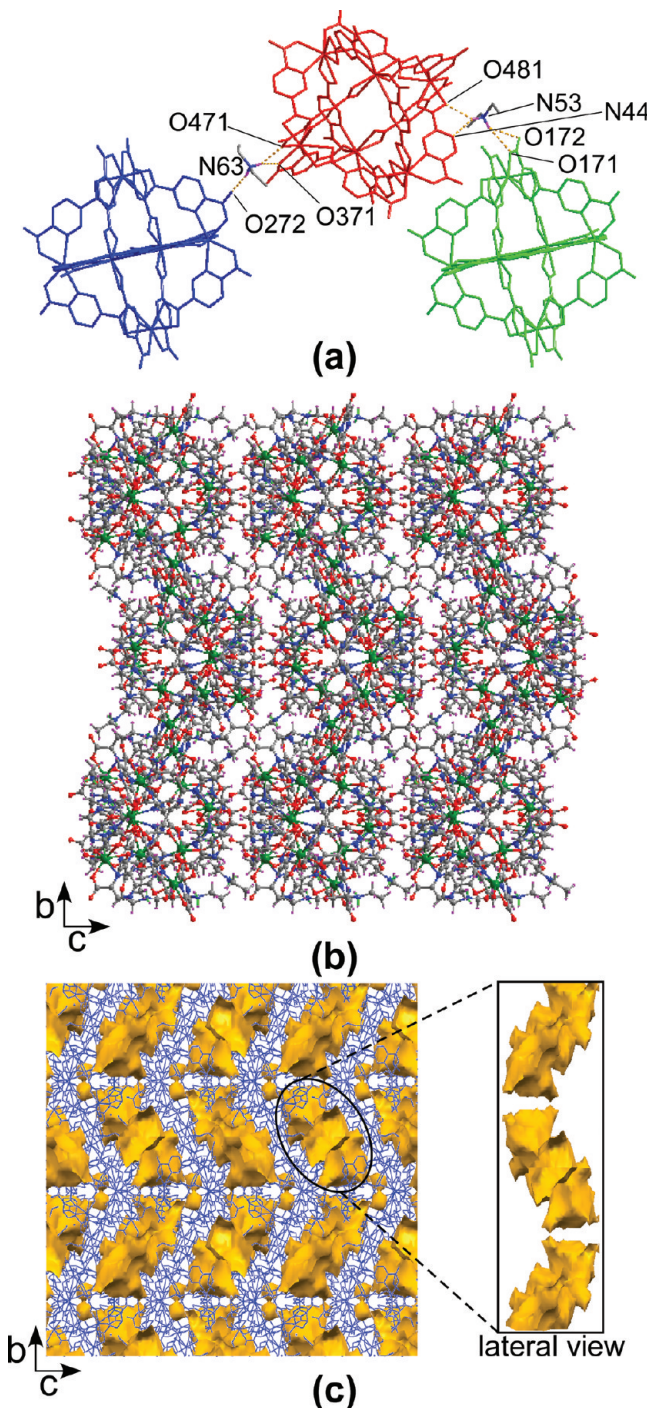


Figure 5. Crystal structure of 2: (a) supramolecular interactions, (b) packing along the *a* axis, and (c) solvent accessible surface (probe radius = 1.4 Å, the organic counterions have not been removed).

oxygen atoms of four bis-chelating pzdc ligands (bridging mode A). The metal coordination polyhedron has a triangular dodecahedron geometry ($S_{DD} = 0.76$) for 3 and a square antiprism geometry ($S_{SAPR} = 0.72$) for 4 (Table 3, Figure 6). The In···In distance through the pzdc bridge is ca. 7.6 Å in both compounds while the In···In···In angles are 129.8° and 73.7° for 3; 137.5° and 84.2° for 4. The junction between the 4-connected tetrahedral building units gives rise to six-member rings that are further linked to build a diamond topological network (dia, sqc6) with the (6⁶) point symbol.

Table 3. Selected Bond Lengths (Å) of Compounds 3–6^a

compound 3			
In1–N1	2.447(3)	In1–O41	2.188(2)
compound 4			
In1–N11	2.475(3)	In1–N21	2.346(3)
In1–O141	2.161(3)	In1–O241	2.226(3)
compound 5		compound 6	
In1–N11	2.286(2)	In1–N11	2.268(3)
In1–O171	2.165(2)	In1–O171	2.103(3)
In1–O181a	2.162(2)	In1–O182b	2.264(3)

^aSymmetry codes: (a) $-y, x - y - 1, z$; (b) $x + 1/2, -y + 1, z + 1/2$.

Although both compounds have the same topological network, their crystal buildings exhibit subtle differences owing to the flexibility of the six-membered rings and the presence of different cations. The network rings are arranged to generate a 2D intersecting channel system that is occupied by crystallization water molecules and the organic cations. The tetramethylammonium cations of compound 3 are only engaged to the anionic framework by electrostatic forces, whereas the disordered diethylammonium cations in 4 are hydrogen-bonded to the carboxylato groups sited in the walls of the channels (O242···H–N33–H···O242), producing something similar to a breathing effect in the metal–organic framework (Figure 7).

Crystal Structures of {(dma)[In(μ-pddc)₂]·xH₂O}_n (5) and {(dma)[In(μ-pddc)₂]_n (6)}. Single-crystals of compound 5 undergo a slow transformation at room temperature accompanied by the release of the crystallization water molecules to render compound 6 (see Supporting Information). Both compounds contain stacked $[In(pddc)₂]_n$ [−] layers that accommodate dimethylammonium cations in between. The anionic layers are comprised of almost planar 4-connected *cis*-InN₂(CO₂)₄ entities (Figure 8) in which the indium atom is coordinated to two nitrogen atoms and four oxygen atoms from two N-/O– chelating moieties and two monocoordinated carboxylate groups of four independent pddc ligands (bridging mode B). Table 3 gathers coordination bond lengths for the chromophores. The coordination polyhedron adopts a trigonal prism geometry in 5 ($S_{TPR} = 1.90$) and an octahedral arrangement in 6 ($S_{OC} = 3.55$).

The chiral *cis*-In(N,O)₂O₂ core presents two enantiomeric forms, Δ and Λ, which coexist in the crystal structures of compounds 5 and 6. The sheets in compound 6 are formed by both enantiomeric forms, whereas the crystal structure of compound 5 presents the alternate stacking of opposite chirality sheets (Figure 9). Another difference within the sheets is the nonchelating carboxylate oxygen atom attached to the metal centers, that is, in the same edge of the N,O-chelate ring in 5 (O181) while is sited in the opposite edge in 6 (O182), resulting in a substantially longer In···In distance [8.9 (6) vs 7.8 Å (5)]. These differences force the assembly of the 4-connected nodes in 5 to generate three- and six-membered windows that are arranged into an overall Kagomé lattice topology (kgm) with the (3²·6²·7²) point symbol, but render a sq1 Shubnikov tetragonal plane net with the (4⁴·6²) point symbol in 6. Moreover, the interlayer separation is substantially longer in the first compound (8.8 Å vs 5.4 Å), where the pddc ligands are arranged outward the mean plane of the sheet.

The piling up of the highly corrugated sheets in compound 5 creates a honeycomb-like pattern with cavities along the crystallographic *c*-axis with diameters ranging from 0.5 to 1.2

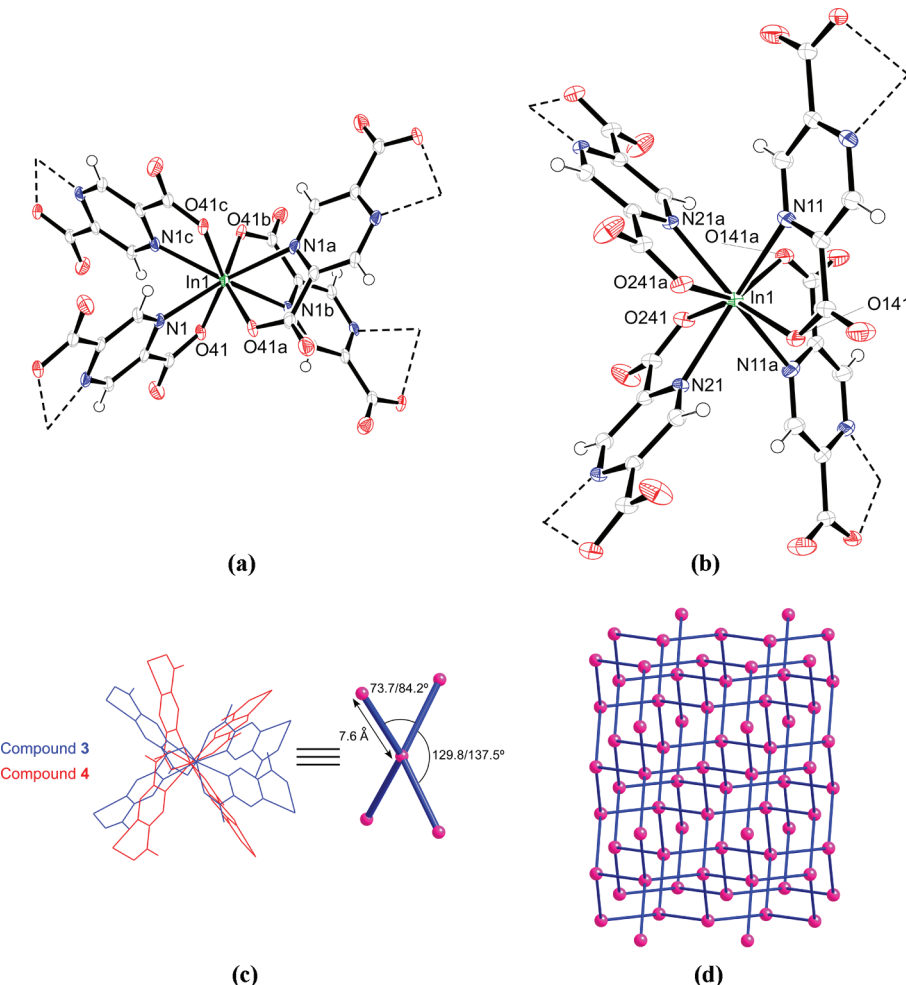


Figure 6. Ortep views of tetrahedral building units (TBU) in (a) 3 and (b) 4. (c) Superposition of TBUs. (d) Topological dia network of both compounds.

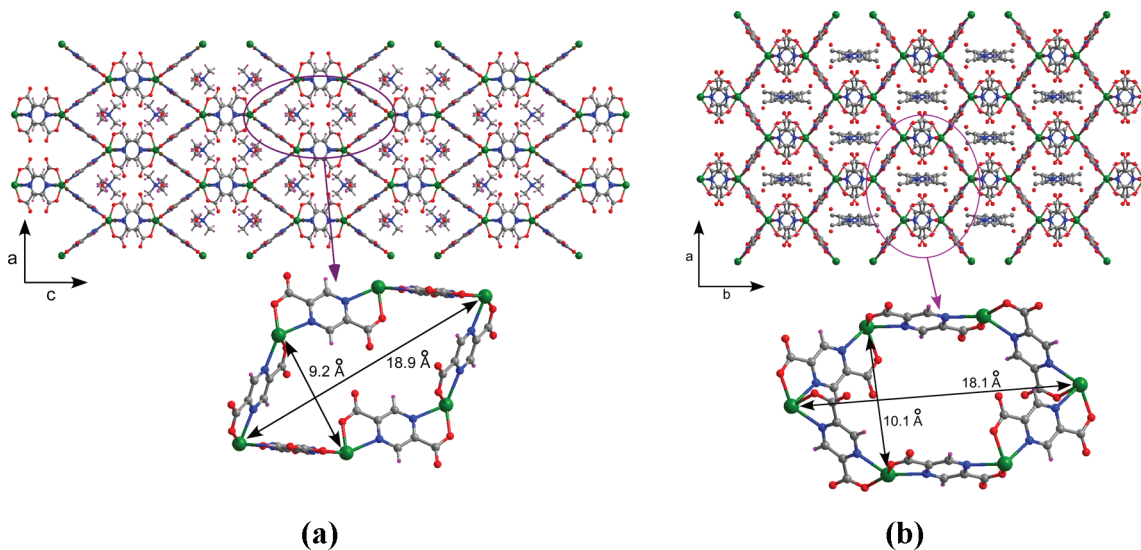


Figure 7. Crystal packing remarking the hexagonal rings in compounds: (a) 3 and (b) 4.

nm (Figure 10) that represent the 36.0% of the unit cell volume. The connectivity between the voids is inhibited by the dimethylammonium cations sited in the interlayer space. The organic cations are disordered into three equivalent positions so their nitrogen atoms point toward the carboxylate oxygen

atoms of the edges of the triangular windows of the Kagomé network of the anionic metal–organic layer. The absence of remarkable interactions between the layers and the release of the crystallization water molecules produces the slow transformation of **5** into the more compact crystal building of

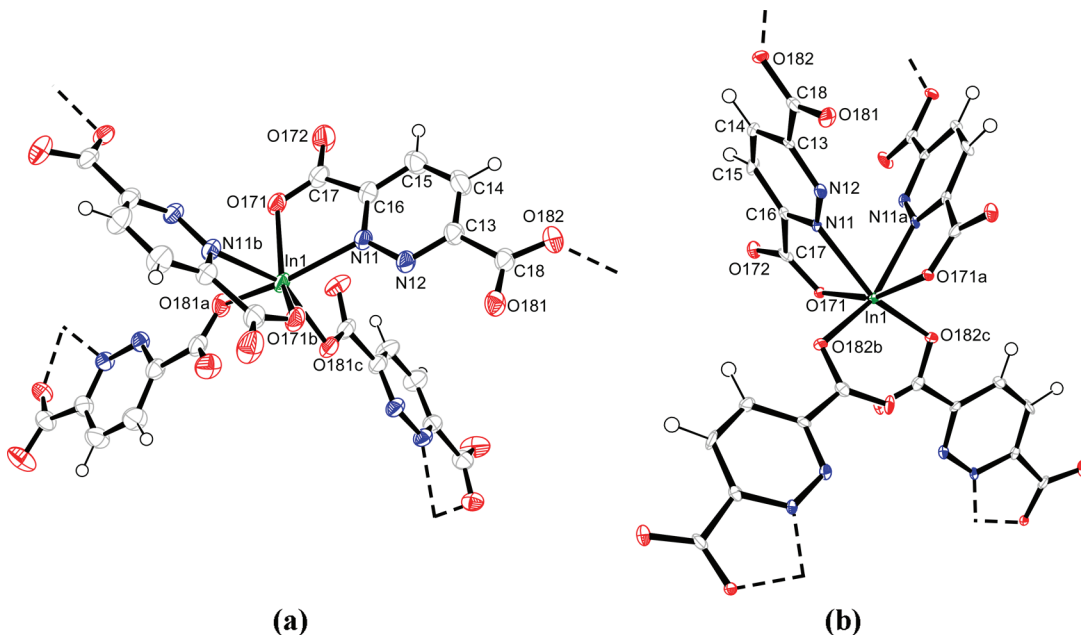


Figure 8. Building units for compounds (a) 5 and (b) 6.

compound 6, which does not show solvent accessible volume, and its 3D cohesiveness is reinforced by the strong anchoring of the dma cations to the adjacent anionic layers through a N22–H···O182 hydrogen bonding interaction.

A careful examination of both crystal structures has allowed us to surmise the mechanism of the solid state transformation described in Figure 11. First, the layers get closer to each other as the interlayer solvent molecules are released. Then, the pddc ligands begin to reorganize inside the *cis*-InN₂(CO₂)₄ building units. The five-member chelate ring remains unchanged but the monocoordinated carboxylate group breaks its coordination bond through the O181 atom, to establish a new connection with a metal center belonging to an adjacent layer by means of the O182 atom. This rearrangement of the crystal structure leads to the generation of new 2D layers containing square rings that are perpendicular to the original ones. A proof of this astonishing change can be observed when comparing the chirality of the metal chromophore within the sheets. In compound 5, each layer consists of the same enantiomer but the presence of a symmetry center between the layers allows the adjacent layer to present opposite chirality. This fact does not happen in compound 6, where every layer consists of alternating Δ and Λ enantiomers. A prolonged exposure of a polycrystalline sample of compound 6 to a water saturated atmosphere does not afford compound 5, but it promotes a partial and reversible transformation to give an unidentified compound with a different X-ray powder diffraction pattern (see Supporting Information).

Structural Description of (dma)₄[In₈(μ-pddc)₁₂(H₂O)₈(OH)₄]·xH₂O (7). Compound 7 consists of open discrete octanuclear metal–organic cages that are connected by means of hydrogen bonding interactions involving the water molecules and the dimethylammonium cations. The centrosymmetric anionic cage is formed by 12 μ-pddc ligands that are sited in the edges of a parallelepipedal cluster and show three different coordination modes (Figure 12). The bis-chelating μ -pddc- $\kappa^2N,O:\kappa^2N',O'$ ligands (mode A in Figure 2) are joined to two indium atoms imposing a distance of ca. 3.9 Å between them along the shorter edge of

the base of the cage. The bis-chelating μ -pddc- $\kappa^2N,O:\kappa^2O',O''$ (mode C) ligands are disposed along the longer edges of the rectangular base of the cage with distances of 8.4 Å. Finally, the bis-monodentated μ -pddc- $\kappa O:\kappa O'$ (mode D) ligands act as pillaring linkers establishing the largest sides of the cage (11.3 Å), in such a way that only two of them expose their endocyclic nitrogen atoms toward the inner cavity of cage. The connectivity in the metal–organic cluster is reinforced by four μ -OH bridges along the shorter edges that are hydrogen bonded to the noncoordinated aromatic nitrogen atoms of the pddc ligands. The coordination of the indium atoms is completed by a water molecule as terminal ligand to give two different N₂O₅ and NO₆ donor sets with distorted pentagonal bipyramidal geometry (S_{PBPY} ranging from 0.75 to 2.39). Selected bond lengths in compound 7 are listed in Table 4.

The octameric entities are interconnected vertex-to-vertex via O_w–H_w···O_{carb} hydrogen bonds and O_w–H_w···O_w–H_w···O_{carb} interactions through a crystallization water molecule (Figure 13). As a result, each cage connects to eight neighboring ones leading to a 3D bcu topological network with the (4²⁴.6⁴) point symbol similar to that found by Sava et al.²² Two dimethylammonium cations are inserted in the hole of the octameric cage and attached to it by means of O_{carb}···H–N–H···N/O_{pddc} interactions. The remaining organic cations are placed among two anionic cages establishing O_{carb}···H–N–H···O_{carb} interactions. This supramolecular arrangement of the anionic and cationic entities gives rise to a 2D intersecting channel system running along the outer space of the cages that represents the 43.9% of the unit cell volume (Figure 14).

CONCLUSIONS

The present work demonstrates that the strategy of combining the In(III) versatile coordination geometry with rigid connectors such as pyrazine-2,5-dicarboxylate and pyridazine-3,6-dicarboxylate in the presence of organic cations provides a tool to direct the dimensionality and connectivity of the anionic MOAs ranging from discrete assemblies to extended frameworks. The synthesis temperature and the hydrogen bonding capacity of the organic cations play a key role in the features of

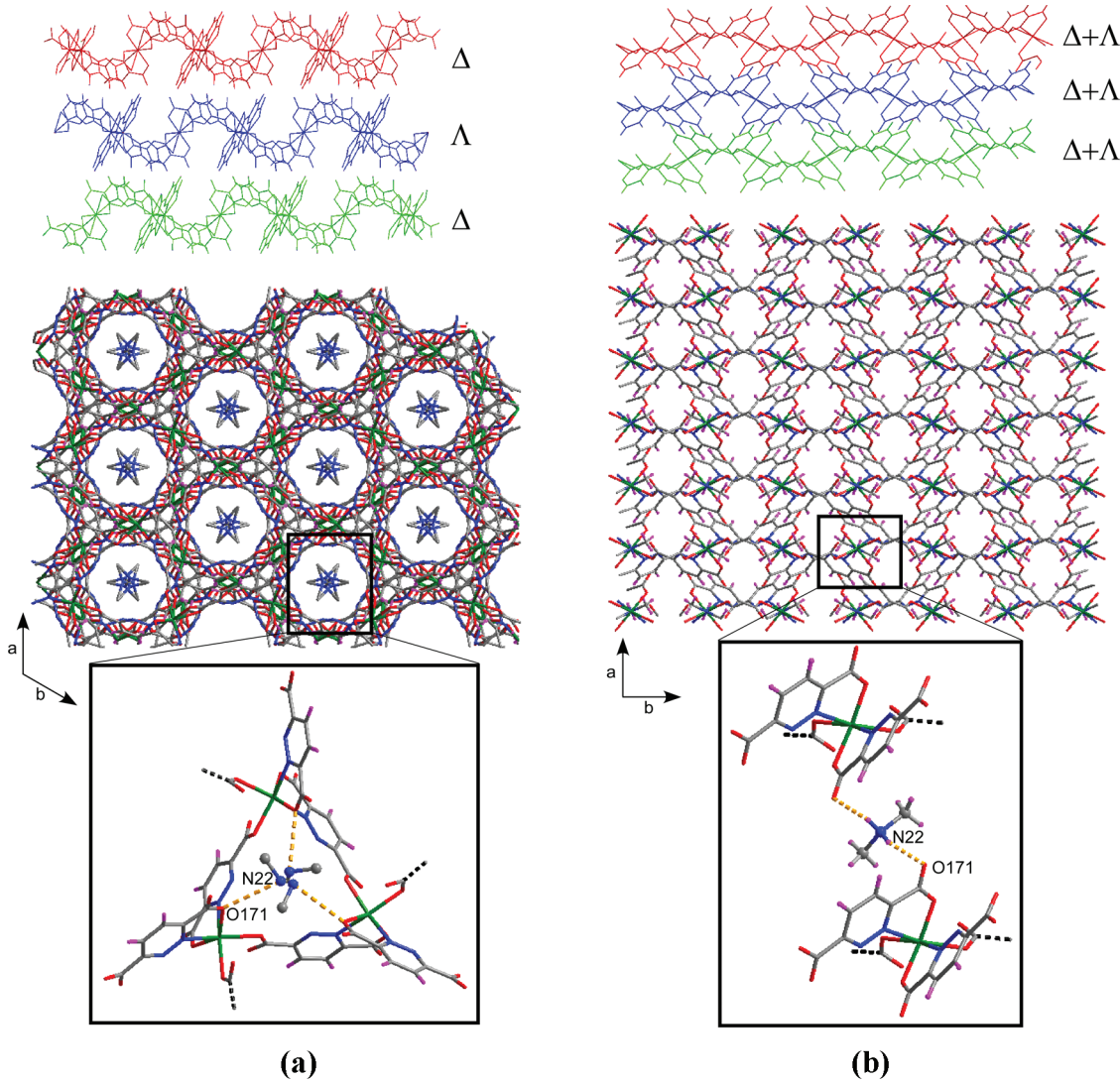


Figure 9. Crystal packing and supramolecular interactions in compounds **5** (a) and **6** (b).

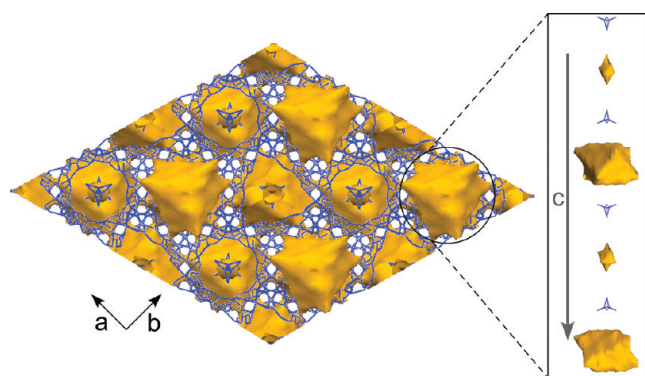


Figure 10. Solvent accessible voids of **5** (probe radius = 1.4 Å, the organic counterions have not been removed).

the anionic metal–organic frameworks in the In/pzdc system. Mild hydrothermal conditions and/or strong hydrogen bonding donor cations shift the self-assembling of the In(III) and pzdc ligands toward hexanuclear discrete anions. At higher reaction temperatures or employing non-hydrogen bonding donor cations, the hexanuclear In/pzdc entities rearrange to give rise to a 3D skeleton. On the other hand, with the analogous

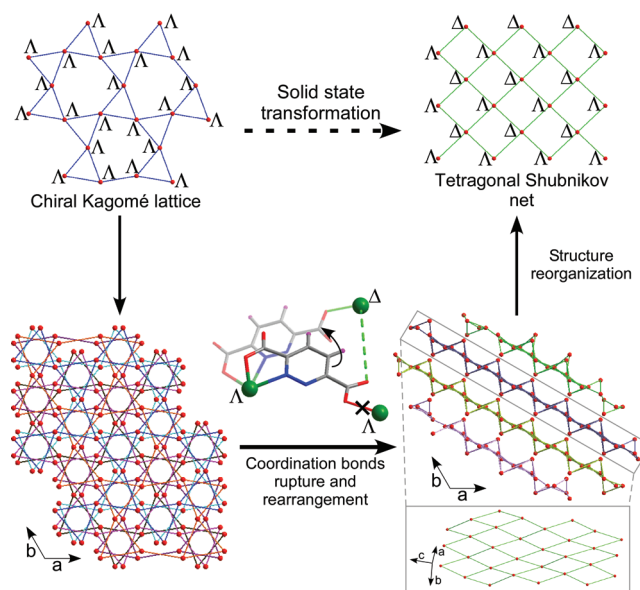


Figure 11. Solid state transformation from **5** to **6** (pddc ligand is represented as a linear connector).

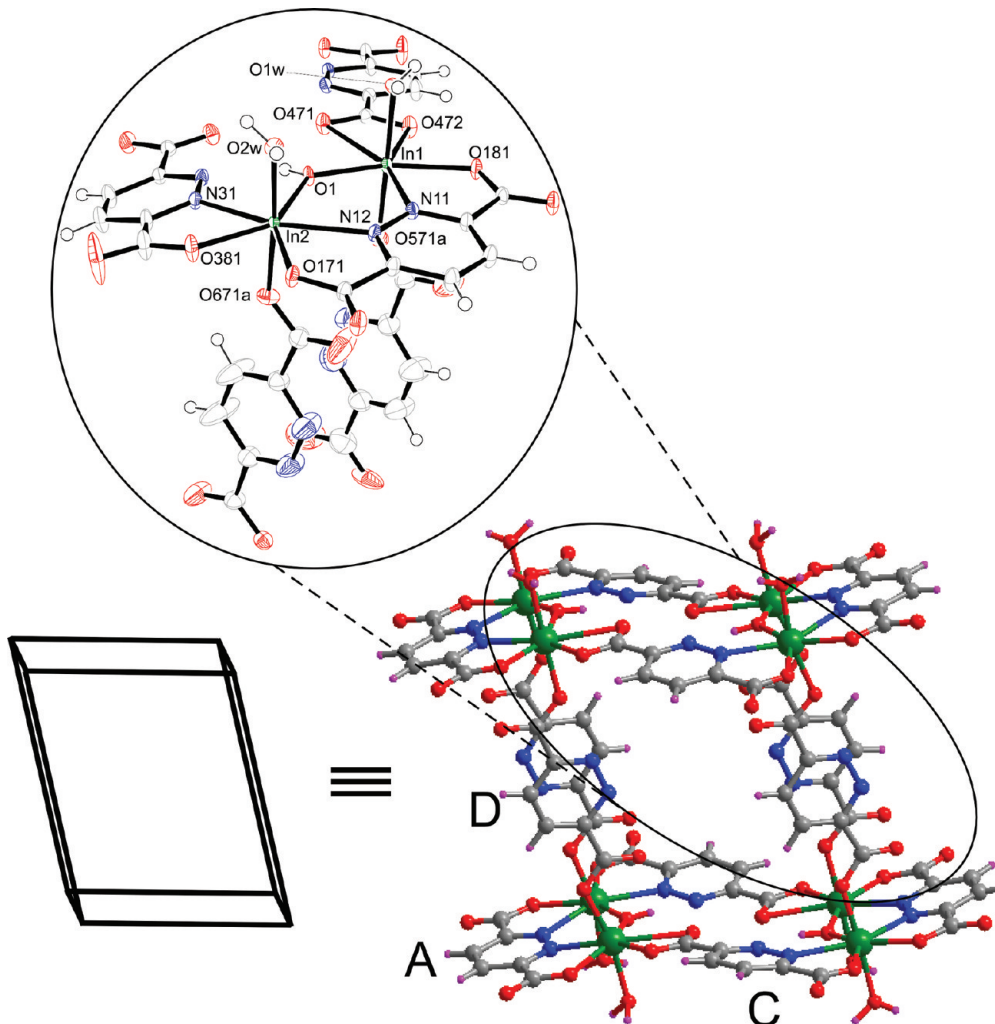


Figure 12. Metal–organic cage in compound 7.

Table 4. Selected Bond Lengths (\AA) of Compound 7^a

In1–N11	2.294(2)	In2–N12	2.432(2)	In3–N21	2.299(2)	In4–N22	2.393(2)
In1–O1	2.073(2)	In2–N31	2.420(2)	In3–O2	2.098(2)	In4–N41	2.437(2)
In1–O181	2.243(2)	In2–O1	2.130(2)	In3–O281	2.165(2)	In4–O2	2.123(2)
In1–O471	2.691(2)	In2–O171	2.270(2)	In3–O371	2.631(2)	In4–O271	2.245(2)
In1–O472	2.153(2)	In2–O381	2.183(2)	In3–O372	2.152(2)	In4–O481	2.207(2)
In1–O571a	2.125(3)	In2–O671a	2.124(2)	In3–O582	2.135(2)	In4–O682	2.116(2)
In1–O1w	2.194(2)	In2–O2w	2.154(2)	In3–O3w	2.170(2)	In4–O4w	2.149(2)

^aSymmetry codes: (a) $-x, -y + 1, -z + 1$.

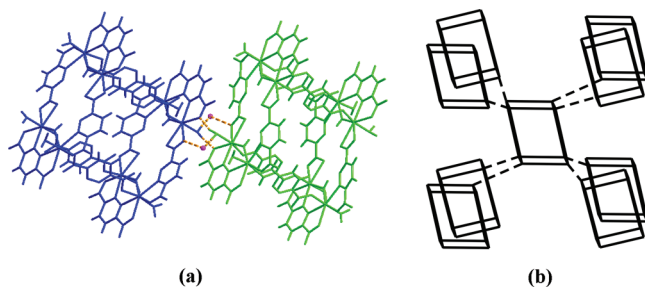


Figure 13. Supramolecular interactions among the cages in 7.

pddc ligand, the amount of water molecules in the reaction media determines the architectural features of the MOAs, since

the gradual increase of its concentration allows the controlled growth of a condensed lamellar structure (**6**), an open anionic lamellar stacking (**5**), and octanuclear anionic entities (**7**).

Compounds showing extended anionic open frameworks (**3**, **4**, and **5**) display channels filled by organic cations that could possess enough freedom of movement to allow their study as potential ionic exchangers. Moreover, the versatility of the studied systems permits us to state that the use of different synthesis conditions and cations of different topology could lead to a great diversity of novel MOAs. The diazinedicarboxylate ligands of these complexes show the predicted most probable coordination modes [**A** (**3**, **4**, and **7**), **B** (**5** and **6**), **C** (**1**, **2**, and **7**) and **D** (**7**)] as they were estimated on the basis of a perusal of the crystallographic information registered in the

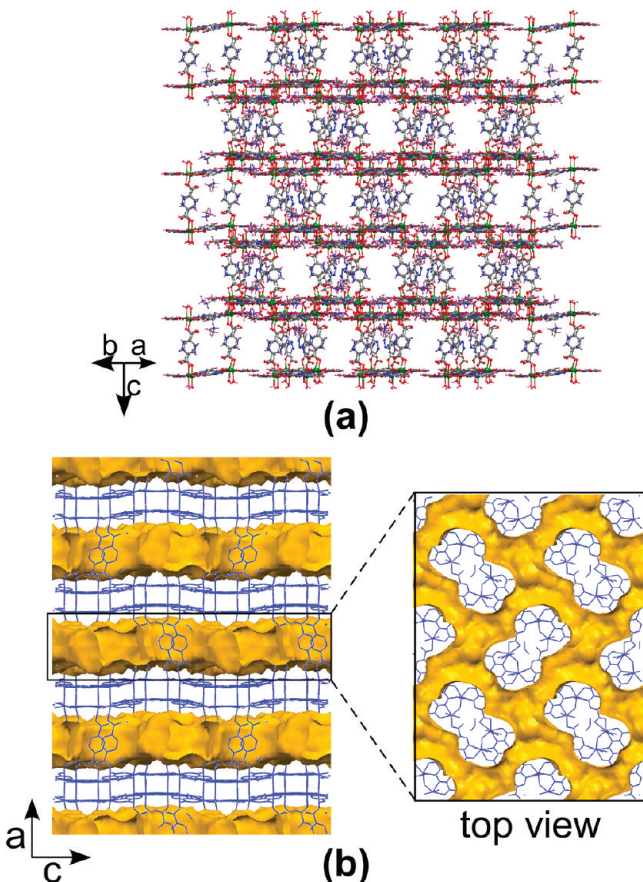


Figure 14. Crystal packing of compound 7 showing the solvent accessible surface.

CSD database, a helpful tool in designing and/or improving of new materials.

ASSOCIATED CONTENT

Supporting Information

Elemental analyses, IR data, XRPD analyses, thermodiffractometric analyses, thermogravimetric measurements, and CIF files. This material is available free of charge via the Internet at <http://pubs.acs.org>.

AUTHOR INFORMATION

Corresponding Author

*E-mail: oscar.castillo@ehu.es (O.C.), garikoitz.beobide@ehu.es (G.B.). Fax: (internat) +34-94601-3500.

Notes

The authors declare no competing financial interest.

ACKNOWLEDGMENTS

Financial support from the Ministerio de Ciencia e Innovación (Project MAT2008-05690/MAT) and the Gobierno Vasco (IT477-10) is gratefully acknowledged. We also thank Universidad del País Vasco/Euskal Herriko Unibertsitatea for predoctoral fellowships (PIFA01/2007/021 and UFI11/53). Technical and human support provided by SGIker (UPV/EHU, MICINN, GV/EJ, ESF) is also acknowledged.

REFERENCES

- (a) Fujiita, M.; Tominaga, M.; Hori, A.; Therrien, B. *Acc. Chem. Res.* **2005**, *38*, 369. (b) Yaghi, O. M.; O'Keeffe, M.; Ockwig, N. W.; Chae, H. K.; Eddaoudi, M.; Kim, J. *Nature* **2003**, *423*, 705.
- (c) MacGillivray, L. R.; Atwood, J. L. *Nature* **1997**, *389*, 469.
- (d) Cheetham, A. K.; Férey, G.; Loiseau, T. *Angew. Chem., Int. Ed.* **1999**, *38*, 3268. (e) Liu, Y. L.; Eubank, J. F.; Cairns, A. J.; Eckert, J.; Kravtsov, V. C.; Luebke, R.; Eddaoudi, M. *Angew. Chem., Int. Ed.* **2007**, *46*, 3278. (f) Moulton, B.; Zaworotko, M. *Chem. Rev.* **2001**, *101*, 1629.
- (g) Férey, G. *Chem. Soc. Rev.* **2008**, *37*, 191. (h) Kitagawa, S.; Kitaura, R.; Noro, S. *Angew. Chem.* **2004**, *116*, 2388.
- (2) (a) Han, S. S.; Choi, S. H.; Goddard, W. A. *J. Phys. Chem.* **2011**, *115*, 3507. (b) Banerjee, R.; Phan, A.; Wang, B.; Knobler, C.; Furukawa, H.; O'Keeffe, M.; Yaghi, O. M. *Science* **2008**, *319*, 939. (c) Morris, W.; Leung, B.; Furukawa, H.; Yaghi, O. K.; He, N.; Hayashi, H.; Houndoungbo, Y.; Asta, M.; Laird, B. B.; Yaghi, O. M. *J. Am. Chem. Soc.* **2010**, *132*, 11006. (d) Liu, S.; Xiang, Z. H.; Hu, Z.; Zheng, X. P.; Cao, D. P. *J. Mater. Chem.* **2011**, *21*, 6649. (e) Wang, B.; Cote, A. P.; Furukawa, H.; O'Keeffe, M.; Yaghi, O. M. *Nature* **2008**, *453*, 207. (f) Li, Z. G.; Wang, G. H.; Jia, H. Q.; Hu, N. H.; Xu, J. W.; Batten, S. R. *CrystEngComm* **2008**, *10*, 983. (g) Zeng, M. H.; Feng, X. L.; Chen, X. M. *Dalton Trans.* **2004**, 2217.
- (3) (a) Chen, B. L.; Xiang, S. C.; Quian, G. D. *Acc. Chem. Res.* **2010**, *43*, 1115. (b) Zhao, D.; Timmons, D. J.; Yuan, D. Q.; Zhou, H. C. *Acc. Chem. Res.* **2011**, *44*, 123. (c) Moulton, B.; Lu, J. J.; Hajndl, R.; Hariharan, S.; Zaworotko, M. J. *Angew. Chem., Int. Ed.* **2002**, *114*, 2945.
- (4) Li, H.; Eddaoudi, M.; O'Keeffe, M.; Yaghi, O. M. *Nature* **1999**, *402*, 276.
- (5) (a) Chen, S. M.; Zhang, J.; Wu, T.; Feng, P. Y.; Bu, X. H. *J. Am. Chem. Soc.* **2009**, *131*, 16027. (b) Lin, Z. Z.; Jiang, F. L.; Chen, L.; Yue, C. Y.; Yuan, D. Q.; Lan, A. J.; Hong, M. C. *Cryst. Growth Des.* **2007**, *7*, 1712. (c) Zheng, S. T.; Zuo, F.; Wu, T.; Irfanoglu, B.; Chou, C. S.; Nieto, R. A.; Feng, P. Y.; Bu, X. H. *Angew. Chem., Int. Ed.* **2011**, *50*, 1849. (d) Liu, Y.; Kravtsov, V.; Larsen, R.; Eddaoudi, M. *Chem. Commun.* **2006**, 1488.
- (6) (a) Guo, Z. G.; Li, Y. F.; Yuan, W. B.; Zhu, X. D.; Li, X. F.; Cao, R. *Eur. J. Inorg. Chem.* **2008**, 1326. (b) Gao, Q.; Jiang, F. L.; Wu, M. Y.; Huang, Y. G.; Chen, L.; Wei, W.; Hong, M. C. *J. Solid State Chem.* **2009**, *182*, 1499. (c) Zheng, S. T.; Bu, J. T.; Li, Y. F.; Wu, T.; Zuo, F.; Feng, P. Y.; Bu, X. H. *J. Am. Chem. Soc.* **2010**, *132*, 17062. (d) Gándara, F.; Gómez-Lor, B.; Gutiérrez-Puebla, E.; Iglesias, M.; Monge, M. A.; Proserpio, D. M.; Snejko, N. *Chem. Mater.* **2008**, *20*, 72. (e) Kim, M. K.; Lee, D. W.; Ok, K. M. *J. Solid State Chem.* **2010**, *183*, 2406. (f) Liu, Y.; Eubank, J. F.; Cairns, A. J.; Eckert, J.; Kravtsov, V. C.; Luebke, R.; Eddaoudi, M. *Angew. Chem., Int. Ed.* **2007**, *46*, 3278. (g) Liu, Y.; Kravtsov, V.; Eddaoudi, M. *Angew. Chem., Int. Ed.* **2008**, *47*, 8446. (h) Vougo-Zanda, Anokhina, E. V.; Duhovic, S.; Liu, L.; Wang, X.; Oloba, O. A.; Albright, T. A.; Jacobson, A. J. *Inorg. Chem.* **2008**, *47*, 4746. (i) Ramaswamy, P.; Hegde, N. N.; Prabhu, R.; Vidya, V. M.; Datta, A.; Natarajan, S. *Inorg. Chem.* **2009**, *48*, 11697.
- (7) (a) Liu, Y. L.; Kravtsov, V. C.; Beauchamp, D. A.; Eubank, J. F.; Eddaoudi, M. *J. Am. Chem. Soc.* **2005**, *127*, 7266. (b) Ramezanipour, F.; Aghabozorg, H.; Shokrollahi, A.; Shamsipur, M.; Stoeckli-Evans, H.; Soleimannejad, J.; Sheshmani, S. *J. Mol. Struct.* **2005**, *779*, 77. (c) Pal, M. K.; Kushwah, N. P.; Wadawale, A. P.; Sagoria, V. S.; Jain, V. K.; Tiekkink, E. R. T. *J. Solid State Chem.* **2007**, *692*, 4237.
- (8) Sava, D. F.; Kravtsov, V. C.; Nouar, F.; Wojtas, L.; Eubank, J. F.; Eddaoudi, M. *J. Am. Chem. Soc.* **2008**, *130*, 3768.
- (9) (a) Beobide, G.; Castillo, O.; Cepeda, J.; Luque, A.; Pérez-Yáñez, S.; Román, P.; Vallejo-Sánchez, D. *Eur. J. Inorg. Chem.* **2011**, *68*. (b) Cepeda, J.; Balda, R.; Beobide, G.; Castillo, O.; Fernández, J.; Luque, A.; Pérez-Yáñez, S.; Román, P.; Vallejo-Sánchez, D. *Inorg. Chem.* **2011**, *50*, 8437. (c) Beobide, G.; Wang, W. G.; Castillo, O.; Luque, A.; Román, P.; Tagliabue, G.; Galli, S.; Navarro, J. A. R. *Inorg. Chem.* **2008**, *47*, 5267. (d) Beobide, G.; Castillo, O.; Luque, A.; García-Couceiro, U.; García-Terán, J. P.; Román, P. *Inorg. Chem.* **2006**, *45*, 5367. (e) Liu, Y.; Kravtsov, V.; Walsh, R. D.; Poddar, P.; Srikanth, H.; Eddaoudi, M. *Chem. Commun.* **2004**, 2806.
- (10) Allen, F. H. *Acta Crystallogr.* **2002**, *B58*, 380.
- (11) Sueur, S.; Lagrenée, M.; Abraham, F.; Bremard, C. *J. Heterocycl. Chem.* **1987**, *24*, 1285.

- (12) (a) *CrysAlisPro*, version 1.171.35.15; Agilent Technologies: Yarnton, UK, 2011. (b) *Stoe & Cie, STADI4 and X-RED*; Stoe & Cie GmbH; Darmstadt, Germany, 2002.
- (13) Altomare, A.; Cascarano, M.; Giacovazzo, C.; Guagliardi, A. *J. Appl. Crystallogr.* **1993**, *26*, 343.
- (14) Sheldrick, G. M. *Acta Crystallogr.* **2008**, *A64*, 112.
- (15) Farrugia, L. J. *J. Appl. Crystallogr.* **1999**, *32*, 837.
- (16) Van der Sluis, P.; Spek, A. L. *Acta Crystallogr.* **1990**, *A46*, 194.
- (17) Spek, A. L. *Acta Crystallogr.* **1990**, *A46*, C34.
- (18) (a) Rodríguez-Carvajal, J. FULLPROF, a Program for Rietveld Refinement and Pattern Matching Analysis. Abstracts of the Satellite Meeting on Powder Diffraction of the XVth Congress of the IUCr, Toulouse, France, 1990; 127. (b) Rodríguez-Carvajal, J. FULLPROF 2000, version 2.5d; Laboratoire Léon Brillouin (CEA-CNRS), Centre d'Études de Saclay, Gif sur Yvette Cedex, France, 2003.
- (19) (a) Lin, J. B.; Xue, W.; Zhang, J. P.; Chen, X. M. *Chem. Commun.* **2011**, *47*, 926. (b) Zhang, J.; Chen, S. M.; Wu, T.; Feng, P. Y.; Bu, X. H. *J. Am. Chem. Soc.* **2008**, *130*, 12882.
- (20) Llunell, M.; Casanova, D.; Cirera, J.; Bofill, J. M.; Alemany, P.; Alvarez, S.; Pinsky, M.; Avnir, D. SHAPE v1.7, University of Barcelona, Barcelona, 2010.
- (21) (a) Blatov, V. A.; Shevchenko, A. P. TOPOS v 4.0, Samara State University, Samara, 2011. (b) Blatov, V. A. *IuCr CompComm. Newsletter* **2006**, *7*, 4.
- (22) Sava, D. F.; Kravtsov, V.; Eckert, J.; Eubank, J. F.; Nouar, F.; Eddaoudi, M. *J. Am. Chem. Soc.* **2009**, *131*, 10394.